coatings

Communication

Testing the Mechanical Properties of High-Strength Zinc-Coated Bolts: FEM Approach

Rafał Grzejda [1,*] and Magdalena Kobielarz [2,3]

[1] Faculty of Mechanical Engineering and Mechatronics, West Pomeranian University of Technology, 19 Piastow Ave., 70-310 Szczecin, Poland
[2] Faculty of Mechanical Engineering, Wroclaw University of Science and Technology, 7/9 Lukasiewicz Str., 50-371 Wroclaw, Poland
[3] Department of Mechanical Engineering, School of Engineering, The University of Western Australia, 35 Stirling Highway, Perth, WA 6009, Australia
* Correspondence: rafal.grzejda@zut.edu.pl

Abstract: High-strength zinc-coated bolts are used as fasteners in prestressed multi-bolted connections. This communication deals with modelling such bolts using the finite element method. The analyses were performed for a zinc-coated M12 HV10.9 bolt. Coatings with the following thicknesses were considered: 40, 60, 84 and 92 μm. The influence of coating thickness on the selected mechanical properties of the bolt was investigated. The corresponding properties of an uncoated bolt were taken as a reference. It is shown that the use of a zinc coating with a standardised thickness is associated with a reduction in bolt stiffness of up to 11.2%.

Keywords: anti-corrosion coatings; galvanising; mechanical properties; high-strength bolts; finite element method

check for updates

Citation: Grzejda, R.; Kobielarz, M. Testing the Mechanical Properties of High-Strength Zinc-Coated Bolts: FEM Approach. *Coatings* **2023**, *13*, 27. https://doi.org/10.3390/coatings13010027

Academic Editor: Jinyang Xu

Received: 28 November 2022
Revised: 19 December 2022
Accepted: 22 December 2022
Published: 23 December 2022

1. Introduction

Bolted connections are often used in many structures exposed to various, including aggressive, environmental conditions [1]. In such cases, the use of anti-corrosion coatings on the bolt surface is indispensable [2,3]. The element most commonly used in the production of anti-corrosion coatings is zinc [4]. The protective durability of zinc coatings is roughly proportional to their thickness [5]. Zinc coating deposition processes are relatively simple and do not require sophisticated equipment, complex technology or large amounts of money [6]. The use of galvanising also brings other benefits. In the case of bolted connections, their use stabilises the coefficient of friction, with no additional lubricant between the threaded parts to be joined. This technique is, therefore, widespread in the automotive industry [7]. It has also been shown that the use of zinc plating on bolts results in a reduced coefficient of friction on the bolt surface compared to black oxidised bolts [8]. The bolt galvanisation methods used in the industry and their brief characteristics are listed below.

Traditional methods of applying zinc coatings are defined in PN-EN ISO 14713-1 [9]. Among these methods, hot-dip galvanising is the most commonly used method for protecting industrial steel components [10–14]. As hot-dip galvanising provides high-quality and long-lasting protection against corrosion, examples of its use can be found in any environment (marine, rural, industrial) and different industry types (shipbuilding, agriculture, engineering). The thickness of coatings deposited on fastener surfaces by hot-dip galvanising is typically in the range of 45 to 65 μm [6,11].

Another method of protecting bolts against corrosion is electro-galvanising, which provides a uniform, thick coating on the fastener surfaces, but with a smaller coating thickness (typically 5 to 15 μm) [11,15]. The corrosion resistance of bolts with such a coating decreases quite rapidly during operation, significantly reducing the service life of the entire multi-bolted structure. The low service life of the coating applied by electro-galvanising is confirmed by Sriraman et al. [16] on the basis of tests carried out for a sheet made of low carbon steel measuring 100 mm by 160 mm and 0.8 mm thick. Based on the depth of wear, the coating life for such sheets was determined to be up to 400 cycles.

A sherardising process also achieves zinc coatings on bolts [17]. It is carried out in closed rotary retorts, where bolts are placed together with zinc powder and zinc oxide. The sherardising process produces 15 to 30 μm thick coatings [11].

In addition to the techniques mentioned above for applying zinc coatings to bolts, mention is also made of thermal diffusion zinc coating technology with reactive atmosphere recirculation. This technology can produce coatings with a thickness of 50 to 72 μm [11].

To conclude the discussion of zinc coatings, it should be noted that there are also methods in which other elements such as tin, aluminium, titanium, copper or lead are added to the galvanised coatings [18–21]. The above indicates that the issue of zinc-based coatings on steel materials is very challenging, still open and worthy of investigation. It is also the subject of this paper, which examines high-strength zinc-coated bolts using the finite element method (FEM), currently the most widely used method in numerical studies [22–27]. The calculations were performed in the Midas NFX 2017 software.

Tests of zinc-coated steel parts with the use of finite element systems have been presented in several papers. Vantadori et al. [21] simulated the bending behaviour of a sheet coated with two layers of zinc using a 2D FE model. Similar studies, but for a 3D FE model, were performed by Kim et al. [28]. Song et al. [29] analysed the surface cracking behaviour of zinc coatings on a steel sheet using a 2D FE model. Kashyzadeh et al. [30] studied the effect of coating thickness on the fatigue life of medium carbon steel specimens, where the results showed a significant fatigue strength reduction rate for increasing coating thickness for galvanised coatings. The authors considered specimens with thicknesses of 13 μm and 19 μm. They used a 2D FE model for the study.

In the literature, however, numerical studies of zinc-coated bolted connections are most often carried out without considering the protective layer. In this way, for example, Pereira et al. [14] investigated the in-service failure of mechanically galvanised low-alloy steel bolted water tanks. Similarly, Tang et al. [31] studied the mechanical characteristics of bolted connections of corrugated steel sheets, while Ajaei and Soyoz [32] analysed the effect of preload deficiency on fatigue demands of wind turbine tower bolts, and Hu et al. [33] simulated the behaviour. Subsequently, Li and Zhan [34] proposed a new joint-slippage model for galvanised steel bolted joints with slippage, while Souto et al. [35] described global–local fatigue approaches for snug tight and preloaded hot-dip galvanised steel bolted joints. Additionally noteworthy is the paper of Tronci and Marshall [36], who studied silver-coated fasteners used in aero-engines. While they used the actual dimensions of the bolt and nut in their analysis, the silver coating was not included as a separate component, and its contact behaviour was taken into account through the pressure-dependent friction coefficient used in the model.

Oechsner et al. [37] noted that zinc coating has a negative effect on the fatigue strength of large-diameter bolts. This conclusion was reached on the basis of experimental studies and analytical calculations. Similar experimental results, but for the AISI 4340 high-strength steel used for fasteners, were reached by Khare et al. [38]. Application of the zinc coating resulted in a yield stress reduction of 2.5% for the steel in the normalised state and of 4.4% for the heat-treated steel. At the same time, a reduction in ultimate tensile stress of 2.1% was obtained for the steel in the normalised state and 3.9% for the heat-treated steel. Glienke et al. [39] carried out tests on HV bolt assemblies for a diameter range from M12 to M64. These tests found a reduction in fatigue strength of approximately 25% for hot-dip galvanised bolts compared to quenched and tempered black bolts. A similar phenomenon was previously noted by Berto et al. [40]. In the cases referred to, the thickness of the zinc coating was not taken into account in the tests. This paper has filled this gap, which describes the effect of zinc coating thickness on the mechanical properties of high-strength zinc-coated bolts. When approaching the modelling of zinc-coated bolts, it was assumed that they could be regarded as a system similar to composite structures, with layers closely adhering to each other [41–46].

2. Materials and Methods

The research subject in this paper is HV bolts with thread size M12 made in mechanical property class 10.9 [47]. The main dimensions of the bolts are shown in Figure 1 and collected in Table 1.

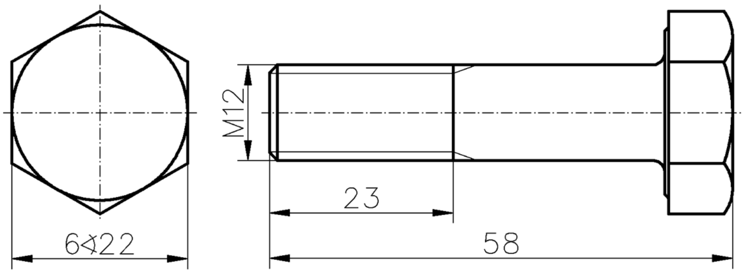

Figure 1. Dimensions of the tested bolts.

Table 1. M12 bolt dimensions [47].

Parameter	Value
Thread diameter, d	12 mm
Thread pitch, P	1.75 mm
Thread flank angle, α	60°
Bearing diameter of the bolt head, d_w	20.5 mm

According to PN-EN ISO 10684 [48], the local coating thickness on HV bolts must be at least 40 µm, while the maximum coating thickness can be 84 µm for a bolt with thread tolerance class 6 h and 92 µm for a bolt with thread tolerance class 6 g, respectively. These guidelines formed the basis for the selection of the set of coating thicknesses analysed in this paper, shown in Table 2. The corresponding properties of an uncoated bolt were taken as a reference.

Table 2. Characteristics of the bolt models.

Model Name	Zinc Coating Thickness [µm]
Model A	–
Model B	40
Model C	60
Model D	84
Model E	92

Following the example of other recent articles using axisymmetric models [49,50], this paper analyses the 2D FE models of the bolt. This approach makes it entirely possible to investigate the influence of the thickness of the zinc coating deposited on the bolt on selected mechanical properties.

The stress–strain behaviour in the elasto-plastic state of bolt materials can be represented by the relationships given in [29,51]:

$$\begin{cases} \sigma = E \cdot \varepsilon & \text{for } \varepsilon \leq \varepsilon_y \\ \sigma = \sigma_y \cdot \left[1 + \frac{E}{\sigma_y} \cdot \left(\varepsilon - \varepsilon_y\right)\right]^n & \text{for } \varepsilon > \varepsilon_y \end{cases} \tag{1}$$

where σ and ε are the actual stress and the true strain, respectively, and where E, σ_y, ε_y and n denote Young's modulus, yield strength, yield strain and work hardening index.

The parameters of the materials used in the bolt model are summarised in Table 3. Values of n were assumed equal to 0.14 for the zinc coating and 0.15 for the steel substrate [29,52].

Table 3. Material properties of the bolt models [53,54].

Material	Young's Modulus, *E* (GPa)	Poisson's Ratio	Yield Strength, σ_y (MPa)	Ultimate Tensile Strength, σ_u (MPa)
Zinc coating	100	0.25	120	145
Steel substrate	210	0.3	900	1000

An example of a zinc-coated FE model is shown in Figure 2. The steel substrate was divided into 2D elements with a maximum side length of 0.1 mm. The steel substrate mesh consisted of 38,470 elements and 39,127 nodes. The zinc coating was divided into 2D elements with a maximum side length of 0.01 mm. The characteristics of the finite element meshes for the zinc-coated models are summarised in Table 4. All bolt models have been formed from 1 mm thick plate elements with a linear shape function. A "welded contact" type connection was used between the finite element meshes for steel and zinc. This is one of the contact types available in the Midas NFX software (Midas NFX 2020 R2, MIDASoft, Inc., New York, NY, USA), allowing elements to be bonded at the initial analysis stage.

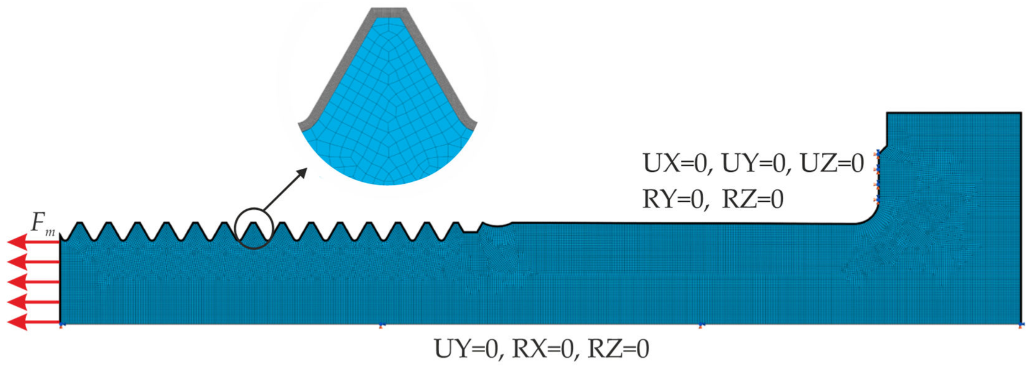

Figure 2. Example of a zinc-coated bolt FE model.

Table 4. Characteristics of the FE mesh for the zinc-coated models.

Model Name	Number of Elements	Number of Nodes
Model B	39,619	49,414
Model C	59,235	69,010
Model D	79,491	89,275
Model E	89,097	98,823

The models were restrained on the axis of symmetry, maintaining the feature of axisymmetry and on the line symbolising the bearing surface of the bolt head. The bolt tension force (the preload F_m) was applied to the face located on the threaded side of the bolt over a length corresponding to the bolt core. The preload force value can be calculated from the relationship [55]:

$$F_m = 0.7 \cdot \sigma_u \cdot A_s \tag{2}$$

where A_s is the nominal stress area of the bolt. F_m for the actual bolt is 59 kN, while that of the 2D FE models of the bolt takes a value equal to 3.45 kN, according to the cross-section of the adopted models.

All calculations were performed using the non-linear statics module in the Midas NFX 2017 software.

3. Results and Discussion

Figure 3 shows the characteristics of axial displacement of the individual bolt models *t* under force F_m in the elastic range of deformation of the materials used for the bolt. At the same time, Table 5 summarises the stiffnesses of the bolt *k* for the adopted models.

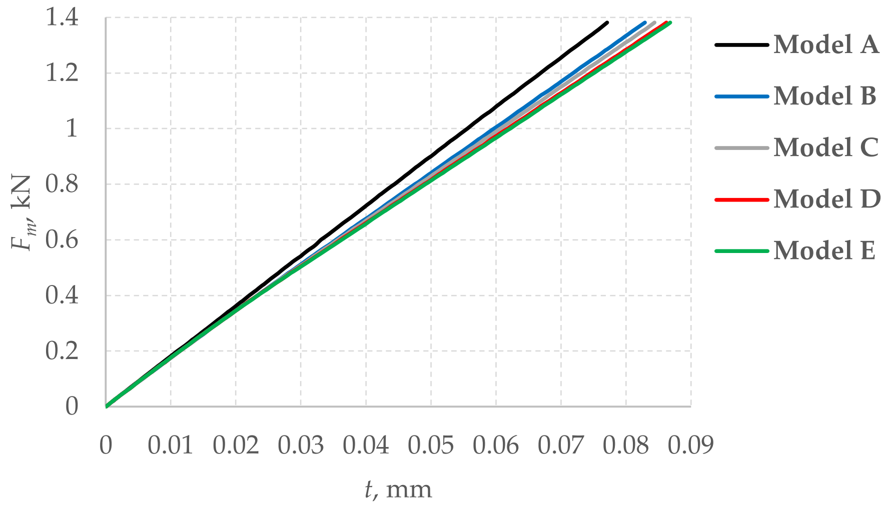

Figure 3. Force–displacement diagrams for the adopted bolt models.

Table 5. Stiffness of the bolt for the adopted models.

Model Name	k, kN/mm	Z, %
Model A	17.90	–
Model B	16.65	7.0
Model C	16.35	8.7
Model D	16.01	10.6
Model E	15.90	11.2

Qualitatively, all characteristics presented in Figure 3 are similar to each other and can all be described as linear. The quantitative analysis of the results shown in Figure 3 was carried out using the Z-indicator, defined as follows:

$$Z = \left| \frac{k_A - k_i}{k_A} \right| \cdot 100 \quad (3)$$

where k_A is the stiffness of the bolt according to model A (uncoated), and k_i is the stiffness of the zinc coated bolt (i = {B, C, D, E}). The Z-indicator values are shown in Table 5.

From the results obtained, it can be concluded that the stiffness of the bolt after zinc coating according to standard [48] can decrease by 7 to 11.2% compared to the stiffness of the bolt without coating. The stiffness of a bolt should be understood as a function of its geometrical parameters (i.e., the cross-section and length of its individual parts) and Young's modulus. The reduction in zinc-coated bolts' stiffness compared to the stiffness of an uncoated bolt is directly related to the reduction in the resultant value of Young's modulus of the uncoated bolt material.

As additional examples of calculation results, Figure 4 shows axial displacement maps for the model without zinc coating and for the model with the thickest zinc coating, respectively.

From the maps summarised in Figure 4, it can be seen that the axial displacement characteristics of the zinc-coated and uncoated bolts are qualitatively similar to each other. In contrast, a quantitative comparison shows that the maximum axial displacement of the bolt with the thickest coating is 20 times greater than that of the bolt without coating.

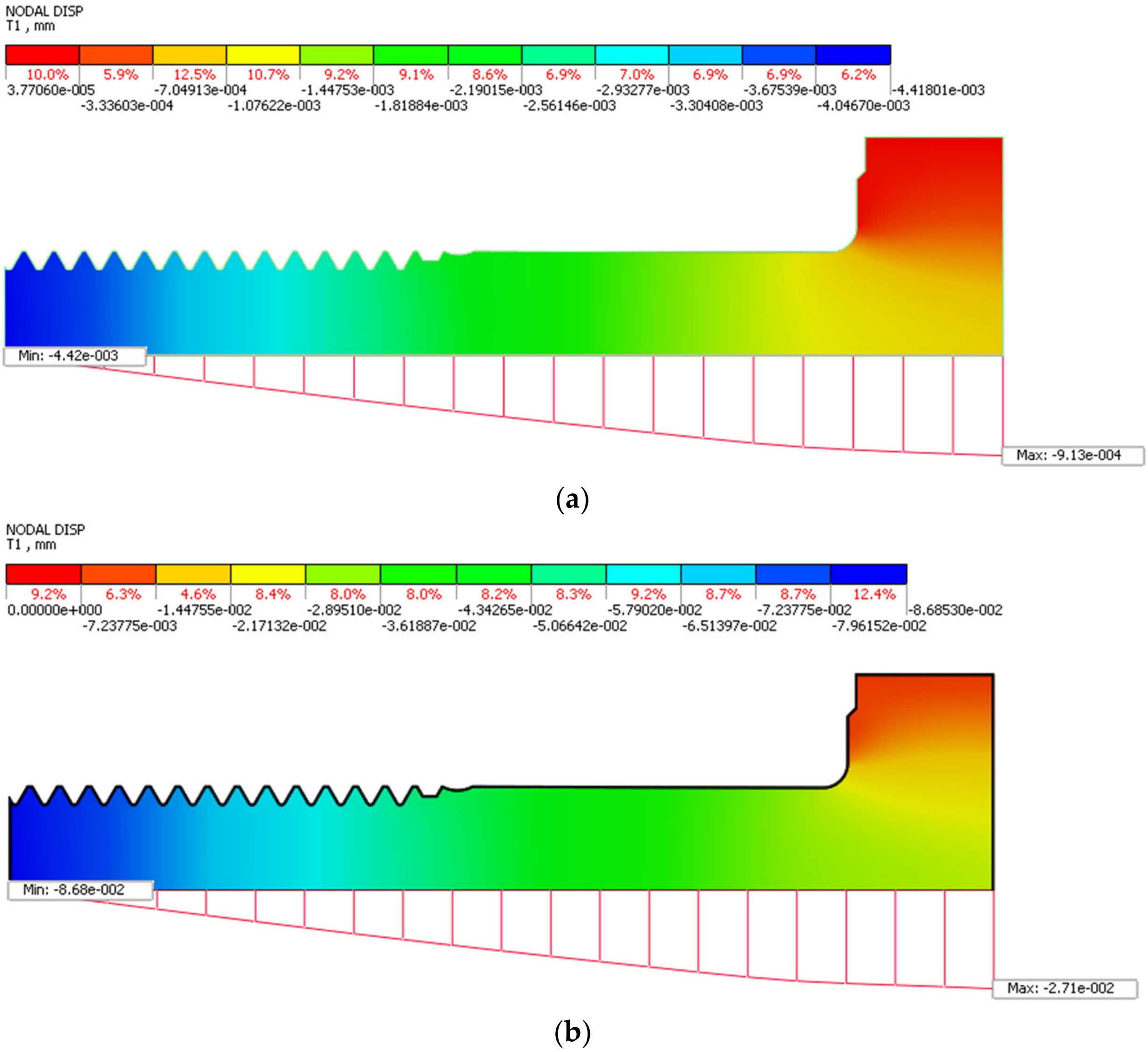

Figure 4. Axial displacement maps in the bolt by: (**a**) model A; (**b**) model E.

4. Conclusions

This communication presents the modelling of high-strength zinc-coated bolts using 2D FE models, and the undertaken work aimed to investigate the effect of zinc coating thickness on selected mechanical properties of the bolt. This issue has not been widely reported in the literature to date. The most important finding of the study is that the stiffness of the bolt after zinc coating can decrease compared to the stiffness of the bolt without coating. It should also be noted that as the zinc coating thickness increases, theoretically as the corrosion resistance increases, the stiffness of bolts may decrease. The conclusions drawn from the calculations warrant further research towards determining the effect of the thickness of different coatings (including multi-coatings [56]) applied to bolts of different sizes and using 3D FE models. One possible direction for such research is to determine a more detailed relationship between mechanical resistance and corrosion resistance of bolts. Another direction could be to investigate the effect of temperature on these resistances [57].

Author Contributions: Conceptualisation, R.G. and M.K.; methodology, R.G.; software, R.G.; validation, M.K.; formal analysis, R.G.; investigation, R.G.; resources, R.G.; data curation, R.G.; writing—original draft preparation, R.G.; writing—review and editing, M.K.; visualisation, R.G.; supervision, R.G.; project administration, R.G.; funding acquisition, R.G. All authors have read and agreed to the published version of the manuscript.

Funding: This research received no external funding.

Institutional Review Board Statement: Not applicable.

Informed Consent Statement: Not applicable.

Data Availability Statement: Not applicable.

Conflicts of Interest: The authors declare no conflict of interest.

References

1. Lachowicz, M.B.; Lachowicz, M.M. Influence of corrosion on fatigue of the fastening bolts. *Materials* **2021**, *14*, 1485. [CrossRef] [PubMed]
2. Votava, J. Anticorrosion protection of strength bolts. *Acta Univ. Agric. Silvic. Mendel. Brun.* **2012**, *60*, 181–188. [CrossRef]
3. Chung, P.P.; Wang, J.; Durandet, Y. Deposition processes and properties of coatings on steel fasteners—A review. *Friction* **2019**, *7*, 389–416. [CrossRef]
4. Dubiel, T.; Balawender, T.; Osetek, M. The fibrous structure of the bolt and its effect on the joint reliability. *Arch. Metall. Mater.* **2021**, *66*, 1075–1085.
5. *PN-EN ISO 1461, 2011*; Hot Dip Galvanised Coatings on Fabricated Iron and Steel Articles, Specifications and Test Methods. Polish Committee for Standardization: Warsaw, Poland, 2011.
6. Jędrzejczyk, D.; Szatkowska, E. The influence of heat treatment on corrosion resistance and microhardness of hot-dip zinc coating deposited on steel bolts. *Materials* **2022**, *15*, 5887. [CrossRef] [PubMed]
7. Grabon, W.A.; Osetek, M.; Mathia, T.G. Friction of threaded fasteners. *Tribol. Int.* **2018**, *118*, 408–420. [CrossRef]
8. Croccolo, D.; De Agostinis, M.; Fini, S.; Olmi, G. Tribological properties of bolts depending on different screw coatings and lubrications: An experimental study. *Tribol. Int.* **2017**, *107*, 199–205. [CrossRef]
9. *PN-EN ISO 14713-1, 2017–08*; Zinc Coatings, Guidelines and Recommendations for the Protection against Corrosion of Iron and Steel in Structures, Part 1: General Principles of Design and Corrosion Resistance. Polish Committee for Standardization: Warsaw, Poland, 2017.
10. Razavi, S.M.J.; Peron, M.; Torgersen, J.; Berto, F.; Mutignani, F. Effect of hot dip galvanisation on the fatigue strength of steel bolted connections. *Frat. Integrità Strutt.* **2017**, *41*, 432–439. [CrossRef]
11. Kania, H.; Sipa, J. Microstructure characterisation and corrosion resistance of zinc coating obtained on high-strength grade 10.9 bolts using a new thermal diffusion process. *Materials* **2019**, *12*, 1400. [CrossRef]
12. Ferraz, G.; Rossi, B. On the fatigue behaviour of hot dip galvanised structural steel details. *Eng. Fail. Anal.* **2020**, *118*, 104834. [CrossRef]
13. Chekirou, F.; Brahimi, K.; Bournine, H.; Hamouda, K.; Haddad, M.; Benkajouh, T.; Le Bot, A. Analysis of the vibrational behavior of a bolted beam in the presence of friction. *Russ. J. Nonlinear Dyn.* **2022**, *18*, 3–18.
14. Pereira, H.B.; Maia, R.R.; Shen, J.; Tong, Q.; de Farias Azevedo, C.R.; Tschiptschin, A.P. In-service failure of mechanically galvanised low alloy steel bolts of three 25,000 m^3 bolted water tanks. *Eng. Fail. Anal.* **2022**, *142*, 106839. [CrossRef]
15. Liu, J.; Ouyang, H.; Peng, J.; Zhang, C.; Zhou, P.; Ma, L.; Zhu, M. Experimental and numerical studies of bolted joints subjected to axial excitation. *Wear* **2016**, *346–347*, 66–77. [CrossRef]
16. Sriraman, K.R.; Strauss, H.W.; Brahimi, S.; Chromik, R.R.; Szpunar, J.A.; Osborne, J.H.; Yue, S. Tribological behavior of electrodeposited Zn, Zn–Ni, Cd and Cd–Ti coatings on low carbon steel substrates. *Tribol. Int.* **2012**, *56*, 107–120. [CrossRef]
17. Almeida, M.E.M. Minimisation of steel atmospheric corrosion: Updated structure of intervention. *Prog. Org. Coat.* **2005**, *54*, 81–90. [CrossRef]
18. Shibli, S.M.A.; Jayalekshmi, A.C.; Remya, R. Electrochemical and structural characterisation of the mixed oxides-reinforced hot-dip zinc coating. *Surf. Coat. Technol.* **2007**, *201*, 7560–7565. [CrossRef]
19. Di Cocco, V.; Iacoviello, F.; Natali, S. Damaging micromechanisms in hot-dip galvanising Zn based coatings. *Theor. Appl. Fract. Mech.* **2014**, *70*, 91–98. [CrossRef]
20. Natali, S.; Volpe, V.; Zortea, L.; Burattini, C.; Di Cocco, V.; Iacoviello, F. Mechanical and structural characterisation of Zn-Ti colored coatings. *Procedia Eng.* **2015**, *109*, 105–112. [CrossRef]
21. Vantadori, S.; Carpinteri, A.; Di Cocco, V.; Fortese, G.; Iacoviello, F.; Natali, S.; Ronchei, C.; Scorza, D.; Zanichelli, A. Novel zinc-based alloys used to improve the corrosion protection of metallic substrates. *Eng. Fail. Anal.* **2017**, *82*, 327–339. [CrossRef]
22. Rusiński, E.; Czmochowski, J.; Pietrusiak, D. Problems of steel construction modal models identification. *Eksploat. Niezawodn. Maint. Reliab.* **2012**, *14*, 54–61.
23. Mandal, B.; Chakrabarti, A. Numerical failure assessment of multi-bolt FRP composite joints with varying sizes and preloads of bolts. *Compos. Struct.* **2018**, *187*, 169–178. [CrossRef]
24. Kaczmarczyk, J.; Kozłowska, A.; Grajcar, A.; Sławski, S. Modelling and microstructural aspects of ultra-thin sheet metal bundle cutting. *Metals* **2019**, *9*, 162. [CrossRef]
25. Łukaszewicz, A. Temperature field in the contact zone in the course of rotary friction welding of metals. *Mater. Sci.* **2019**, *55*, 39–45. [CrossRef]

26. Borawski, A.; Tarasiuk, W.; Borawska, E.; Szczucka-Lasota, B.; Krzysztoforski, M. Evaluation of the influence of the percentage of copper content on the physical and chemical properties of the friction material. *Transp. Probl.* **2020**, *15*, 29–38. [CrossRef]
27. Belardi, V.G.; Fanelli, P.; Vivio, F. Analysis of multi-bolt composite joints with a user-defined finite element for the evaluation of load distribution and secondary bending. *Compos. Part B Eng.* **2021**, *227*, 109378. [CrossRef]
28. Kim, S.I.; Her, J.U.; Jang, Y.C.; Lee, Y. Experimental and finite element analysis for fracture of coating layer of galvannealed steel sheet. *Trans. Nonferrous Met. Soc. China* **2011**, *21* (Suppl. S1), s111–s116. [CrossRef]
29. Song, G.M.; Sloof, W.G.; Pei, Y.T.; De Hosson, J.T.M. Interface fracture behavior of zinc coatings on steel: Experiments and finite element calculations. *Surf. Coat. Technol.* **2006**, *201*, 4311–4316. [CrossRef]
30. Kashyzadeh, K.R.; Arghavan, A. Study of the effect of different industrial coating with microscale thickness on the CK45 steel by experimental and finite element methods. *Strength Mater.* **2013**, *45*, 748–757. [CrossRef]
31. Tang, G.; Yin, L.; Guo, X.; Cui, J. Finite element analysis and experimental research on mechanical performance of bolt connections of corrugated steel plates. *Int. J. Steel Struct.* **2015**, *15*, 193–204. [CrossRef]
32. Ajaei, B.B.; Soyoz, S. Effects of preload deficiency on fatigue demands of wind turbine tower bolts. *J. Constr. Steel Res.* **2020**, *166*, 105933. [CrossRef]
33. Hu, Y.; Shen, L.; Nie, S.; Yang, B.; Sha, W. FE simulation and experimental tests of high-strength structural bolts under tension. *J. Constr. Steel Res.* **2016**, *126*, 174–186. [CrossRef]
34. Li, B.; Zhan, Y. A new joint-slippage model for galvanised steel bolted joints with slippage. *Structures* **2021**, *34*, 1034–1047. [CrossRef]
35. Souto, C.D.S.; Gomes, V.M.G.; Da Silva, L.F.R.C.; Figueiredo, M.V.; Correia, J.A.F.O.; Lesiuk, G.; Fernandes, A.A.; De Jesus, A.M.P. Global-local fatigue approaches for snug-tight and preloaded hot-dip galvanised steel bolted joints. *Int. J. Fatigue* **2021**, *153*, 106486. [CrossRef]
36. Tronci, G.; Marshall, M.B. Understanding the behaviour of silver as a low friction coating in aerospace fasteners. *Tribol. Int.* **2016**, *100*, 162–170. [CrossRef]
37. Oechsner, M.; Beyer, J.; Simonsen, F.; Schaumann, P.; Eichstädt, R. Experimental and analytical assessment of the fatigue strength of bolts with large dimensions under consideration of boundary layer effects. In Proceedings of the MATEC & 2nd ESTAD 2015 European Steel Technology and Application Days, Düsseldorf, Germany, 15–19 June 2015.
38. Khare, A.; Dwivedi, S.K.; Vishwakarma, M.; Ahmed, S. Experimental investigation of hydrogen embrittlement during coating process and effect on mechanical properties of high strength steel used for fasteners. *Mater. Today Proc.* **2018**, *5*, 18707–18715. [CrossRef]
39. Glienke, R.; Schwarz, M.; Marten, F.; Eichstädt, R.; Schwerdt, D.; Meyer, M.; Dörre, M. On fatigue strength of large-size bolt-assemblies in steel constructions under consideration of manufacturing and surface condition related impacts—Part 2: Evaluation of fatigue tests. *Stahlbau* **2022**, *91*, 20–38. (In German) [CrossRef]
40. Berto, F.; Mutignani, F.; Guido, E. Effect of hot dip galvanisation on the fatigue behaviour of steel bolted connections. *Int. J. Fatigue* **2016**, *93*, 168–172. [CrossRef]
41. Kozuń, M.; Kobielarz, M.; Chwiłkowska, A.; Pezowicz, C. The impact of development of atherosclerosis on delamination resistance of the thoracic aortic wall. *J. Mech. Behav. Biomed. Mater.* **2018**, *79*, 292–300. [CrossRef]
42. Wysmulski, P.; Debski, H. Post-buckling and limit states of composite channel-section profiles under eccentric compression. *Compos. Struct.* **2020**, *245*, 112356. [CrossRef]
43. Szachogluchowicz, I.; Sniezek, L.; Slezak, T.; Kluczyński, J.; Grzelak, K.; Torzewski, J.; Fras, T. Mechanical properties analysis of the AA2519-AA1050-Ti6Al4V explosive welded laminate. *Materials* **2020**, *13*, 4348. [CrossRef]
44. Borawski, A. Impact of operating time on selected tribological properties of the friction material in the brake pads of passenger cars. *Materials* **2021**, *14*, 884. [CrossRef] [PubMed]
45. Rozylo, P.; Wysmulski, P. Failure analysis of thin-walled composite profiles subjected to axial compression using progressive failure analysis (PFA) and cohesive zone model (CZM). *Compos. Struct.* **2021**, *262*, 113597. [CrossRef]
46. Borawski, A. Testing passenger car brake pad exploitation time's impact on the values of the coefficient of friction and abrasive wear rate using a pin-on-disc method. *Materials* **2022**, *15*, 1991. [CrossRef] [PubMed]
47. *PN-EN 14399-4, 2015–04*; High-Strength Structural Bolting Assemblies for Preloading, Part 4: System HV, Hexagon Bolt and Nut Assemblies. Polish Committee for Standardization: Warsaw, Poland, 2015.
48. *PN-EN ISO 10684, 2006*; Fasteners, Hot Dip Galvanised Coatings. Polish Committee for Standardization: Warsaw, Poland, 2006.
49. Zhang, W.; Xie, J.; Li, T.; Ding, Y. Tensile low-cycle fatigue performance and life prediction of high-strength bolts. *J. Constr. Steel Res.* **2022**, *197*, 107468. [CrossRef]
50. Shakeri, I.; Danielsen, H.K.; Tribhou, A.; Fæster, S.; Mishin, O.V.; Eder, M.A. Effect of manufacturing defects on fatigue life of high strength steel bolts for wind turbines. *Eng. Fail. Anal.* **2022**, *141*, 106630. [CrossRef]
51. Dao, M.; Chollacoop, N.; Van Vliet, K.J.; Venkatesh, T.A.; Suresh, S. Computational modeling of the forward and reverse problems in instrumented sharp indentation. *Acta Mater.* **2001**, *49*, 3899–3918. [CrossRef]
52. Shisode, M.P.; Hazrati, J.; Mishra, T.; de Rooij, M.B.; van den Boogaard, A.H. Semi-analytical contact model to determine the flattening behavior of coated sheets under normal load. *Tribol. Int.* **2020**, *146*, 106182. [CrossRef]
53. *PN-EN 1993-1-8, 2006*; Eurocode 3: Design of Steel Structures, Part 1–8: Design of Joints. Polish Committee for Standardization: Warsaw, Poland, 2006.

54. Zinc and Its Uses. Available online: https://www.azom.com/article.aspx?ArticleID=749 (accessed on 12 November 2022).
55. Grzejda, R. FE-modelling of a bolted lap connection using a simplified bolt model. *Model. Eng.* **2017**, *31*, 24–28.
56. Duarte, T.; Meyer, Y.A.; Osório, W.R. The holes of Zn phosphate and hot dip galvanizing on electrochemical behaviors of multi-coatings on steel substrates. *Metals* **2022**, *12*, 863. [CrossRef]
57. Saeedikhani, M.; Blackwood, D.J. Finite element method for thin film corrosion modelling: Where we advanced and where we would like to advance? *Corros. Mater. Degrad.* **2020**, *1*, 273–281. [CrossRef]